Supplemental Material

Persistent high polarization of excited spin ensembles during light emission in semiconductor quantum-dot–well hybrid nanosystems

Kazuki Takeishi,[1] Satoshi Hiura,[1] Junichi Takayama,[1] Kodai Itabashi,[1] Masayuki Urabe,[1] Akihiro Washida,[1] Takayuki Kiba,[2] and Akihiro Murayama[1,*]

[1]*Graduate School of Information Science and Technology, Hokkaido University, Kita 14, Nishi 9, Kita-ku, Sapporo 060–0814, Japan*

[2]*Kitami Institute of Technology, 165 Koen-cho, Kitami 090–8507, Japan*

A. Coupled excited states in the coupled QD-QW structures and the effects of multiple dot coupling 2

B. Time-evolution of circular polarization property at the QD ground state ....…………………… 4

A. Coupled excited states in the coupled QD-QW structures and the effects of multiple dot coupling

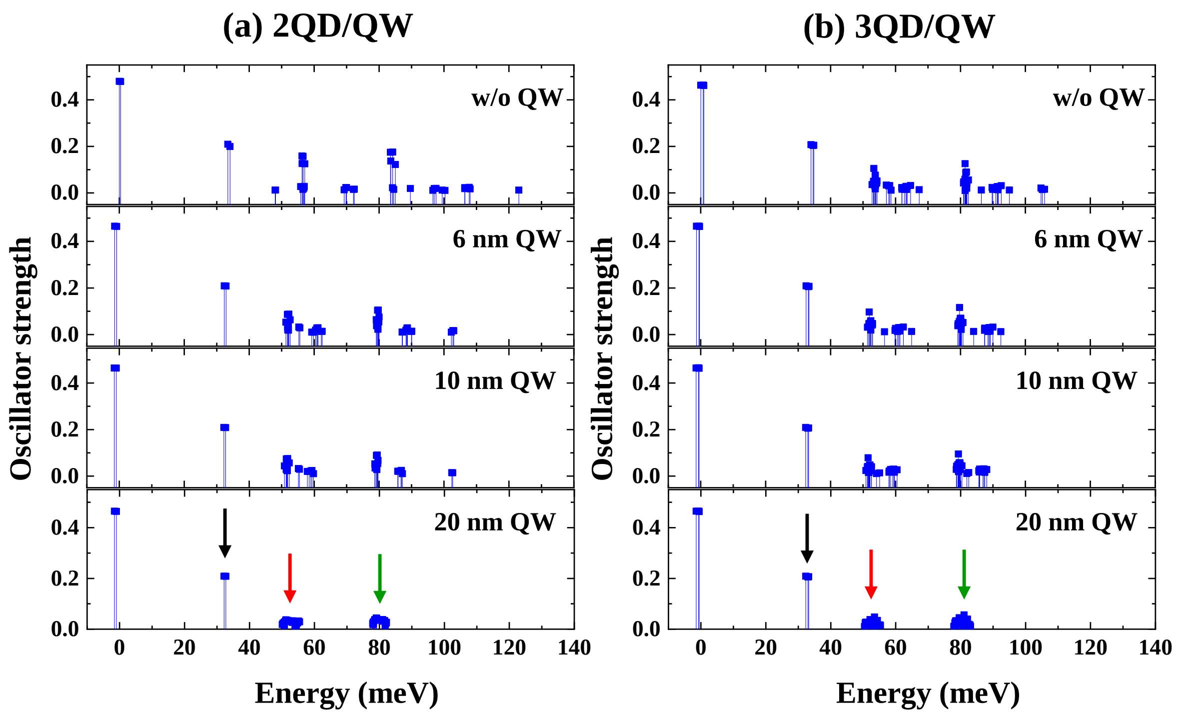

FIG. S1. Oscillator strength as a function of recombination energy between an electron and a hole for the coupled QD-QW samples based on two (a) or three (b) QDs with different QW thicknesses, where the horizontal axis indicates the recombination-energy difference from the ground-state energy in weakly coupled QDs without a QW (top panel; w/o QW). Black, red, and green arrows indicate the excited states (see text).

Detailed calculations of electron and hole wavefunctions in the coupled QD-QW structures revealed energy-level structures. The oscillator strength as a function of the recombination energy between an electron and a hole are plotted in Fig. S1, for various QD-QW samples based on two or three QDs with different QW thicknesses. An excited state identified by a black arrow in the figure is observed at approximately 32 meV above from the ground state of weakly coupled QDs without a QW (top panel), which is composed of s-like electron and d-like hole states. However, this transition is not usually observed because the d-band of these holes is not occupied due to the many energetically lower p-like states. The excited states, indicated by the red arrow, at 50-60 meV above the ground state are responsible for the time-resolved PL detected in Fig. 2, and therefore expressed as the 1st ES in Fig. 4(a) for the rate-equation analysis, in which one of the p-like electron states and p-like hole states are recombined. The accumulation of these transitions can increase the oscillator strength since each transition spectrum is significantly broadened due to the structural inhomogeneities of the self-assembly grown dots. The significant spectral red-shit of the ground state PL peak is observed in the 20 nm-thick QW sample as shown in Fig. 2(c), which can be attributed to the electron localization via stronger inter-dot coupling in the inhomogeneous dot ensemble in addition to the weakened confinements. The nature of the coupling and its strength, i.e., the spatial distribution of the electron wavefunction, are not shown. These aspects can be discussed in detail from each calculation result of the wavefunction. For instance, the oscillator strength of these coupled excited states (red arrow; 1st ES) for the 20 nm-thick QW sample appears to be weaker than those of in the other samples. In these cases, the electron wavefunction spreads significantly over 2 dots while the hole wavefunction is strongly localized at a single dot due to its heavier effective mass. These many-coupled states, which originate from various hole-states are responsible for the measured spin transfer and are subsequently discussed in this study. The radiative lifetimes at the excited states are also affected by the coupling of electron wavefunctions. We can quantitatively estimate effects of the coupling on the lifetime based on the above oscillator strength, as compared to the radiative decay time of 0.6 ns at the ground state. The estimated values distribute between 2 and 10 ns at the 1st ES in the 20 nm-thick QW sample, depending on the coupling strength. However, the other samples including the single QD sample without the QW show similar broad distribution, as suggested in the above Fig. S1. These lifetimes are significantly longer than the PL decay times at the excited states around 0.2 ns, typically as shown in Fig. 3(c). Therefore, non-radiative processes are dominant and taken into account in our rate-equation analysis.

In addition, higher-energy coupled states exist, i.e., at approximately 80 meV above the ground state as indicated by the green arrow in Fig. S1. However, the direct contribution of these higher-energy coupled states to the spin-transfer phenomenon is unclear in this study. Energy relaxation from these higher-energy coupled states (green arrow) to the former coupled states (red arrow) occurs. This process is too fast to be detected by means of time-resolved PL using our streak camera. The spin transfer through the higher-energy coupled states can be significantly suppressed by this ultrafast energy relaxation to the lower-energy coupled states. If the samples are excited with much higher excitation powers, the higher-energy coupled states will play an important role in the spin transfer because of the significant state filling of the lower-energy coupled states.

Then, we expanded the aforementioned 2 dot-based model to a 3 dot-based model as shown in Fig. S1 (b), where 3 dots were arranged to be ideally aligned along a lateral direction as the simplest case. The energy structures of those coupled excited states appear to be similar to those in the 2 dot model, except for the weakly coupled QDs without a QW (top panel). However, the fine structure is modified because of the more complicated coupling interactions among the 3 dots. This information can provide further insight into multiple coupling states among dots with many energy splitting. The real situation is expected to be rather complicated and impossible to estimate precisely because of the inhomogeneous dot separation caused by the current self-assembly dot growth. These multiple and inhomogeneous dot coupling may form band-like transfer paths.

B. Time-evolution of circular polarization property at the QD ground state

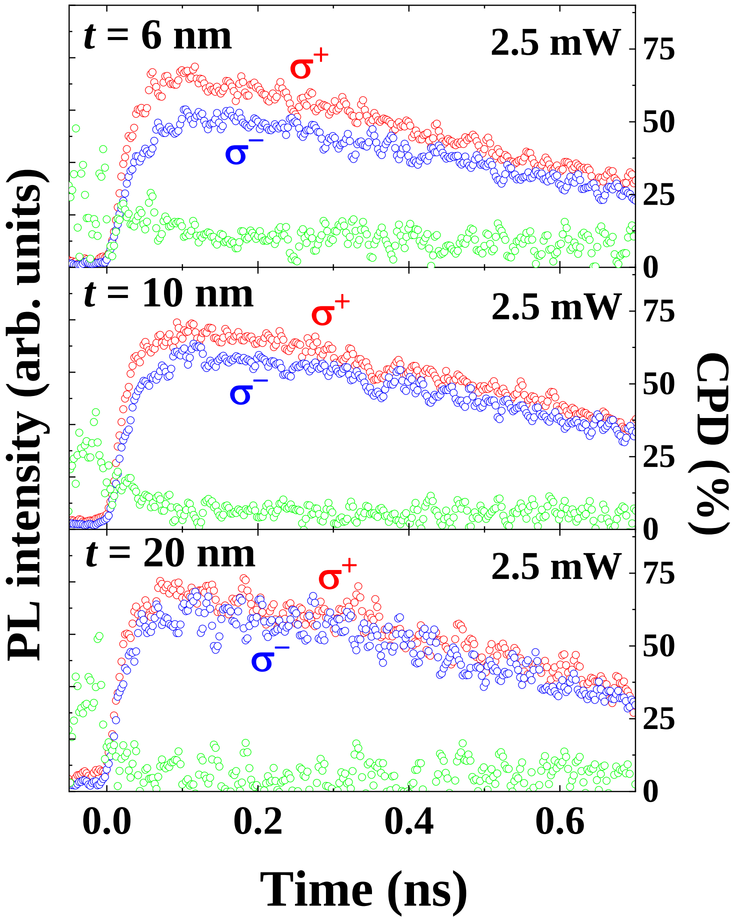

Fig. S2 PL decay profiles with σ^+ (co-circular; red open circle) and σ^- (cross circular; blue open circle) polarizations as a function of the QW thickness t at the ground state of the QD ensemble in coupled QD-QW structures. The CPD value (green open circle) as a function of time is also plotted.

Time-dependent and circularly polarized PL intensities are shown in Fig. S2. We tuned the excitation power to 2.5 mW, which represents the lowest excitation value that can generate sufficiently meaningful data quality, although the PL intensity detected was weak because of the detection sensitivity of the streak camera. It can be observed that the rise of the PL intensity is slower than that of the excited states as shown in Fig. 2. This results from the ground-state observation via many energy-relaxation paths with various relaxation times. Also, the PL decay property after the PL-intensity maximum an approximately 0.1 ns is not steep and exhibits a “plateau-like” behavior which is characteristic of the state filling. The limited density of the ground states induces this state filling at the present excitation power. The degree of circular polarization (CPD) decays rapidly or close to zero, which can be affected by this state filling. Majority spin states can immediately be occupied because of the lower density of the ground states. The subsequent continuous injection of the majority spin is then blocked.

In contrast, minority spins which originate from many spin-relaxation processes at excited states can be injected until their states are fully occupied. As a result, the development of circular polarization is significantly suppressed, which is referred to as Pauli's spin blocking. After solving the state filling for the majority spin due to radiative recombination later than 0.5 ns, identical PL decaying properties are observed among all samples with a radiative decay time of 0.6 ns.

We can observe an enhancement of the CPD value with a decrease of the QW thickness from almost zero for the case of the 20 nm-thick QW to about 10 % for that of the 6 nm-thick QW. This can reflect the spin transfer dynamics at excited coupled states. In the latter case of the 6 nm QW, photo-excited spin-polarized electrons relax from the excited states to the ground state and are localized within each QD (intra-dot relaxation) with a significantly weaker inter-dot spin-transfer effect. That is, CPD can be observed as a result of the usual spin injection into the QD ground state after spin relaxation at the excited states, and then decreased by spin relaxation within this ground state itself. The abovementioned state filling effect on the CPD dynamics can also degrade the CPD values. In contrast, spins are efficiently transferred among excited coupled states in the dot ensemble and subsequently relax to individual ground states that are localized at each dot in the 20 nm-thick QW. This was discussed with respect to Figs. 4-6. In this case, the minority spins can be efficiently injected from the excited coupled states into the minority-spin states of the ground states, shortly after the occupancy of the majority spin. Therefore, the ground states show very low or almost zero spin polarization. As a result, the spin polarization of the excited coupled states are filtered and efficiently enhanced, as we previously indicated. Therefore, the time evolution of circular polarization, i.e., spin polarization, support spin-transfer dynamics which result in persistent high spin polarization of the excited coupled states.